Preparation and Properties of Ag-Based Electrical Contact Material Reinforced by Ti_3AlC_2 Ceramic and its Derivative $Ti_3C_2T_x$

Jianxiang Ding
Southeast University https://orcid.org/0000-0001-7365-373X
Kaige Zhang
Anhui University of Technology
Xiao Zhang
Anhui University of Technology
Kuankuan Ding
Anhui University of Technology
Xinxin Xia
Anhui University of Technology
Dongming Liu
Anhui University of Technology
Songlin Ran
Anhui University of Technology
Chengjian Ma
Yancheng Institute of Technology
Wei Zheng
Southeast University
Peigen Zhang (zhpeigen@seu.edu.cn)
Southeast University
Zhengming Sun
Southeast University

Research Article

Keywords: metal-ceramic composite, MAX phase ceramic, 2-D MXene, microstructure, conductivity, mechanical property, arc erosion resistance

Posted Date: July 1st, 2021

DOI: https://doi.org/10.21203/rs.3.rs-659958/v1

Abstract

As a new kind of two-dimensional carbide material, $Ti_3C_2T_x$ has revealed its exceptional potentials in many applications. Herein, we successfully prepared the Ag/$Ti_3C_2T_x$ composite by powder metallurgy and investigated its comprehensive properties by compared with Ag/Ti_3AlC_2 composite. The Ag/$Ti_3C_2T_x$ was found to possess the 29% lower resistivity(30×10^{-3} μΩ·m) than Ag/Ti_3AlC_2(42×10^{-3} μΩ·m) and excellent machinability with intermediate hardness (64 HV), showing broad application prospect as non-toxic electrical contact materials. The improved conductivity of Ag/$Ti_3C_2T_x$ composite is attributed to the metallicity of $Ti_3C_2T_x$ itself, the good interface bonding between the $Ti_3C_2T_x$ and Ag, and the microstructural features rendered by the deformability of $Ti_3C_2T_x$. Although the arc erosion resistance of Ag/$Ti_3C_2T_x$ needs to be further improved, it is a powerful and potential alternative material for the Ag/CdO in the further.

Highlights

1. Ag matrices reinforced by Ti_3AlC_2 and $Ti_3C_2T_x$ were successfully obtained with powder metallurgy.
2. Stripe-like $Ti_3C_2T_x$ uniformly distributes in Ag and shows smaller cross-sectional area.
3. Ag/$Ti_3C_2T_x$ shows good conductivity, machinability, and moderate arc erosion resistance.
4. Superior conductivity results from stronger metallicity of $Ti_3C_2T_x$, and good interface bonding of Ag /$Ti_3C_2T_x$.
5. Lack of Al-Ag diffusion hinders improving arc erosion resistance of Ag/$Ti_3C_2T_x$ contact materials.

Introduction

As the critical component in low-voltage switching device, Ag-based electrical contacts are widely applied in contactor, breaker and relay, etc. Service life of these devices largely depend on the properties of the electrical contact material[1]. The conventional material “Ag/CdO” has long been preferred because of its outstanding contacting and arc extinction properties since middle of last century. However, the toxicity of CdO causes serious pollution problems, restricting its applications[2]. In the past few decades, Cd-free electrical contact materials, such as Ag/SnO_2, Ag/ZnO, Ag/C, Ag/Ni, have been studied extensively[3–7]. These substitutes cannot yet emulate Ag/CdO in terms of temperature rise, contact resistivity, machinability, arc erosion resistance, etc. Therefore, environment-friendly alternative with properties matching up CdO is of high demand.

Over the past decades, *MAX* phase[8–10], combining excellent properties of metal and ceramic, has been widely investigated in various fields[11–16]. As a representative member of *MAX* family, Ti_3AlC_2 has been used to reinforce Ag matrix as the electrical contact material[17–21]. However, the electrical resistivity of the Ag/Ti_3AlC_2 composite is not satisfactory, which is initially attributed to the inter-diffusion between Al

layer and Ag matrix[22]. 2011, Y. Gogotsi and W.M. Barsoum jointly obtained a new kind of carbide material($Ti_3C_2T_x$) with two-dimensional(2-D) structure, coined as *MXenes*[23, 24], were produced by selectively etching off Al atom planes from its parent Ti_3AlC_2. To date, $Ti_3C_2T_x$ has received great attentions of many applications[25–29]. In addition to large specific surface area, $Ti_3C_2T_x$ has good electrical conductivity, thermal-conducting property, and hydrophilicity[30], and thus it is promising reinforcement for electrical conductive composite. Especially, $Ti_3C_2T_x$ has demonstrated its potential as an additive in composites with polymers(PVA, PAM, PEI, PAN etc.), ceramics(MoS_2, TiO_2 etc.) and carbon materials(CNT, MWCNT, CNFs etc.)[31]. Hence, the electric conductive $Ti_3C_2T_x$ is expected to reinforce Ag matrix as a new electrical contact material.

In this study, the application of 2-D *MXene* to electrical contact material is explored. $Ti_3C_2T_x$ reinforcing Ag-based composite was prepared by powder metallurgy, and its overall properties, such as electrical resistivity, hardness, machinability, tensile strength, and anti-arc erosion were investigated and compared with those of Ag-based composite reinforced by Ti_3AlC_2 ceramic. The mechanism of properties difference of the both samples were also analyzed and concluded. The research results would provide significant data for the design and preparation of the new generation of environment-friendly silver-ceramic composite electrical contact materials in the future.

Experimental

Base materials for composites were Ag(99.9%, ~ 10 μm) and Ti_3AlC_2(99.0%, ~ 10 μm). $Ti_3C_2T_x$ was obtained by immersing Ti_3AlC_2(5 g) into hydrofluoric acid(HF) solution(100 mL, 40 wt%) for 24 h under magnetic stirring(40°C)[23]. Ag/10 wt%$Ti_3C_2T_x$(Ag/$Ti_3C_2T_x$) and Ag/10 wt%Ti_3AlC_2(Ag/Ti_3AlC_2) mixtures were individually homogenized by ball milling for 0.5 h according to the mass ratio. These two mixtures were subsequently cold-pressed into green bodies(15 mm in diameter, 2 mm in thickness) under 800 MPa, and then heat treated at 700°C for 2 h in argon atmosphere.

Phase composition of the samples was characterized by X-ray diffraction(XRD, Bruker-AXS D8, Germany). The structure change of Ti_3AlC_2 and $Ti_3C_2T_x$ powders were further characterize by Transmission Electron Microscopy(TEM)(FEI, Nova Nano 450, America).Vickers hardness of samples was tested by the micro-hardness tester(FM-700, Future-Tech Corp., Japan). Resistivity of samples was measured by the four probe method(Metra HIT 27 I, Gossen Metrawatt, Germany). Microstructure and chemical compositions were characterized by a scanning electron microscope(SEM, FEI/Philips Sirion 2000, Netherlands), equipped with an energy dispersive spectrometer (EDS, AZtes X-MAX 80). The tensile strength of both samples were tested at a universal test machine(AGS-X5kN, SHIMADZU, Japan) with a speed of 1 $mm \cdot min^{-1}$. Finally, the Ti_3AlC_2-reinforcing and $Ti_3C_2T_x$-reinforcing Ag-based composite electrical contact were installed in commercial contactors and tested under the harsh condition(400V/100A/AC3, GB14048.4-2010) at Low Voltage Switch Testing Center of Shanghai Electrical Appliance Research Institute.

Results And Discussion

Fig. 1 shows the phase compositions and microstructures of raw powders(Ti_3AlC_2 and $Ti_3C_2T_x$). Ti_3AlC_2 was characterized by the granular morphology with smooth surfaces(Fig. 1a), and $Ti_3C_2T_x$ exhibited a multilayered morphology with the layer thickness of 0.15~0.37 μm(Fig. 1b). Fig. 1b obviously shows that the(002) diffraction peak of $Ti_3C_2T_x$ is tilted towards low angle, which also confirms the expansion of $Ti_3C_2T_x$ layer space.

Fig.2 shows the different microstructural characteristics of Ti_3AlC_2 and $Ti_3C_2T_x$. Ti_3AlC_2 particle displays a smooth margin at the bright field TEM images(Fig. 2a), but the margin of $Ti_3C_2T_x$ particle after etching takes flakiness morphology(Fig.2c). Fig. 2b displays the high resolution transmission electron microscope(HRTEM) image of Ti_3AlC_2 corresponding to the [100] crystal band axis direction. There is a layer of Al atoms between every three layers of Ti atoms, and the distance between the two Al layers is 1.115 nm. HRTEM image indicates that the Al layer is almost completely etched out of Ti_3AlC_2(Fig. 2d), and the distance of three Ti layers increase to 1.651 nm. The TEM results are consistence with those of XRD and SEM results, and further confirms the structural difference between Ti_3AlC_2 and its derivative $Ti_3C_2T_x$.

The microstructures and element distributions of Ag/Ti_3AlC_2 and Ag/$Ti_3C_2T_x$ composites are displayed in Fig. 3. As shown in Fig. 3a and Fig. 3b, both reinforcements(Ti_3AlC_2 and $Ti_3C_2T_x$) uniformly distribute in Ag matrices, Ti_3AlC_2 retains the granular morphology while $Ti_3C_2T_x$ takes the stripe-shaped morphology. Fig. 3(c-j) displays the element distributions of Ag, Ti and Al in composites, which further confirms that Ti_3AlC_2 and $Ti_3C_2T_x$ take different shapes in Ag matrices. Moreover, slight diffusion of Al with Ag is observed in Ag/Ti_3AlC_2(Fig. 3f), while a few Al element is detected in Ag/$Ti_3C_2T_x$(Fig. 1l), which is consistent with the XRD and TEM results.

Contact materials are usually manufactured into various shapes, necessitating excellent machinability. A typical negative case is SnO_2 whose high hardness leads to the poor machinability of Ag/SnO_2, which hinders its substitute to CdO[32]. Fig. 4 shows the Vickers hardness of Ag/$Ti_3C_2T_x$, Ag/Ti_3AlC_2, and pure Ag(for reference). Ag/$Ti_3C_2T_x$ possesses intermediate hardness(64 HV), and can be cut into different shapes, including rod, rivet, disc and square(the insert in Fig. 4). The good machinability originates from the 2D structure of $Ti_3C_2T_x$, in which weak van der Waals interaction exists between layers. In addition, contacts usually carry high current density in service, thus a low resistivity is a prerequisite to potential electrical contact materials. As shown in Fig. 4, the Ag/$Ti_3C_2T_x$ and Ag/Ti_3AlC_2 composites own low resistivity(16×10^{-3} μΩ·m of Ag). In particular, the resistivity of Ag/$Ti_3C_2T_x$(30×10^{-3} μΩ·m) is 29% lower than that of Ag/Ti_3AlC_2(42×10^{-3} μΩ·m), which is very meaningful for the practice application.

The improved conductivity of Ag/$Ti_3C_2T_x$ can be explained from three aspects: higher conductivity of $Ti_3C_2T_x$ than that of Ti_3AlC_2, enhanced interface bonding between Ag and $Ti_3C_2T_x$, deformability of the

stripe-shaped $Ti_3C_2T_x$ in Ag matrix.

Firstly, based on the first-principle band structure calculations, in Ti_3AlC_2, Ti 3*d* state contributes the majority of the total densities of states(DOS) at Fermi level; removal of the Al layers from Ti_3AlC_2 results in the redistribution of Ti 3*d* states from broken Ti-Al bonds into delocalized Ti-Ti metallic-like bonding states, leading to the increase of local DOS maximums at Fermi level[33]. Thus, in *MXene*($Ti_3C_2T_x$), the electron density of states near Fermi level($N(E_f)$) is 1.9~3.2 times higher than that in the corresponding *MAX*(Ti_3AlC_2)[34]. Secondly, EDS mapping indicates the existence of O and F elements, which may come from the functional groups(-F, -OH) of $Ti_3C_2T_x$ surface[35](Fig. 5a). Generally, the hydrophilicity of -F/-OH functional groups is beneficial to the bonding between $Ti_3C_2T_x$ and metal matrix[34], which avoids the similar phenomenon of poor interface bonding between carbon nanotubes, fibers and metal matrix[36]. In addition, the SEM observation also displays the tight bonding between $Ti_3C_2T_x$ and Ag matrix without cracks and holes, as shown in Fig. 3b and Fig. 3g. Hence, the uniform microstructure and good bonding of Ag/$Ti_3C_2T_x$ improved the conductivity. Thirdly, as shown in Fig. 3c, 3g, the microstructure of stripe-shaped $Ti_3C_2T_x$ is obviously different from that of granular Ti_3AlC_2 in Ag matrix. The 2D layered structure of $Ti_3C_2T_x$ facilitates its deformability during preparation. The $Ti_3C_2T_x$ were cold compacted into stripe-like $Ti_3C_2T_x$(average thickness of ~3 microns), whereas Ti_3AlC_2 retains its original shape(average diameter of ~10 microns). Fig. 5b and 5c schematically illustrate the relationship between the electron transmission and the shape of reinforcements in composites. In contrast with granular Ti_3AlC_2, stripe-shaped $Ti_3C_2T_x$ has smaller cross-sectional area perpendicular to the current direction, minimizing the scattering section for electrons and the resistance to the electron transmission. In summary, the excellent machinability and electrical conductivity makes Ag/$Ti_3C_2T_x$ a promising substitute to Ag/CdO.

However, as shown in Fig. 6, the maximum tensile strength of Ag/$Ti_3C_2T_x$ composite(32.77 MPa) is far less than that of Ag/Ti_3AlC_2 composite(145.52 MPa). The superior tensile strength of Ag/Ti_3AlC_2 composite derives from the interdiffusion between active Al atomic layer with Ag matrix. On the contrary, the absence of Al layer leads to the weaker interface bonding strength between $Ti_3C_2T_x$ and Ag matrix, which finally deteriorates the mechanical property of entire Ag/$Ti_3C_2T_x$ composite.

In order to further investigate the property of Ag/$Ti_3C_2T_x$, electrical arc discharging experiment were carried out on this contact surface under a harsh condition(AC-3, 100A, 400V, GB14048.4-2010). The Ag/$Ti_3C_2T_x$ contact failed to make and break after 1233 arc discharging. The optical image shows that the shape of contact remains well with some dents and protuberances(Fig. 7a, 7b). The surface morphologies of Ag/$Ti_3C_2T_x$ contact after arc erosion are subsequently exhibited in Fig. 7c, complete edge and flat surface were further confirmed by SEM. Some Ag spheres, solidified Ag blocks, and small cracks were observed at high-magnification SEM image(Fig. 7d). Fig. 7e-7h exhibit the microstructure and chemical composition of Ag/$Ti_3C_2T_x$ contact surface. There are many irregular dark block surrounded by little bright particles(Fig. 7e). As shown in Fig. 7f, area 1(dark block) contains large amount of Ti, O, F with

trace of Ag and Al, which may be attributed to the Ti-O-F mixture produced by electrical arc erosion to $Ti_3C_2T_x$. Area 2(bright particles) mainly composes of Ag, F, and O. It is deduced that the Ag-O-F mixture were produced by the absorption of O_2 in liquid Ag and reaction with -F function group of $Ti_3C_2T_x$. Fig. 7h displays two types of spheroid particles at magnified SEM image. EDS analysis results show that both the particles contained vast N element, which indicated that these two particles compose of Ag-O-F-N.

The relative mass loss of Ag/$Ti_3C_2T_x$(54% after 1233 times arc discharging) is considerably more than that of Ag/Ti_3AlC_2(0.82% after 3000 times arc discharging), which is also attributed to the absence of Al layer in Ti_3AlC_2. As analyzed previously, the lack of Al-Ag interdiffusion leads to the weak bonding strength of $Ti_3C_2T_x$ with Ag, and thus decrease the mechanical property of composite, which accordingly impairs the resistance to electrical arc impact damage. In addition, the absence of Al-Ag interdiffusion also results in the poor wettability of $Ti_3C_2T_x$ with Ag during electrical arc discharging and consequently decrease viscosity of molten pool, finally deteriorating the resistance to the material transfer of $Ti_3C_2T_x$ and Ag under electrical arc high-temperature. Nonetheless, there is still space for the further improvement of the arc erosion resistance of Ag/$Ti_3C_2T_x$ with superior electrical conductivity by the composition design, structure optimization, technique promotion in the following work.

Conclusions

In this work, Ag-based electrical contact material, reinforced by Ti_3AlC_2 ceramic and its 2D derivative carbide($Ti_3C_2T_x$), was successfully prepared by powder metallurgy. The microstructure, chemical composition, hardness, conductivity, machinability, mechanical property and are erosion resistance of Ag/Ti_3AlC_2 and Ag/$Ti_3C_2T_x$ composites were investigated and compared. The main conclusions are as follows:

1. $Ti_3C_2T_x$ uniformly distributes in Ag matrix in stripe-like shape.
2. In contrast with Ag/Ti_3AlC_2, Ag/$Ti_3C_2T_x$ has lower resistivity(30×10^{-3} μΩ·m), which is 29% lower than that of Ag/Ti_3AlC_2. The superior conductivity of Ag/$Ti_3C_2T_x$ results from the stronger metallicity of $Ti_3C_2T_x$, uniform microstructure and the good interface bonding between $Ti_3C_2T_x$ and Ag matrix, and smaller cross-sectional area of $Ti_3C_2T_x$ in Ag-based composite.
3. The moderate hardness and excellent machinability of Ag/$Ti_3C_2T_x$ are also satisfactory when it is utilized as electrical contact materials.
4. The tensile property(32.77 MPa) of Ag/$Ti_3C_2T_x$ composite is inferior to that of Ag/Ti_3AlC_2(145.52 MPa) due to the lack of Al-Ag interdiffusion.
5. Ag/$Ti_3C_2T_x$ shows moderate arc erosion resistance with production of Ti-O-F, Ag-O-F, and Ag-O-F-N mixture, which is inferior to that of Ag/Ti_3AlC_2, but the improved space is huge in future.

Declarations

Acknowledgements

This work is supported by Anhui Provincial Natural Science Foundation(No. 2008085QE195), Youth Research Foundation of Anhui University of Technology(No. QZ201903), National Natural Science Foundation of China(Grant Nos. 51731004; 52072003, 52002347), National Key Research and Development Program of China(No.2017YFE0301403), Jiangsu Planned Projects for Postdoctoral Research Funds(No. 2020Z158) and Natural Science Foundation of Jiangsu Province(No. BK20201283), Open Foundation of Key Laboratory of Ministry of Education(Anhui University of Technology, No. GFST2020KF04). The authors are thankful to Dr. Chengjian Ma for the help with SEM and TEM analysis.

References

1. F. Fehim, U. Huseyin, Microstructure, hardness and electrical properties of silver-based refractory contact materials[J], Materials & Design, 2003, **24**(7): 489-492.
2. F. Hauner, D. Jeannot, K. McNeilly, J. Pinard, Advanced $AgSnO_2$ contact materials for the replacement of AgCdO in high current contactors[C]. Proceedings of the Forty-Sixth IEEE Holm Conference on Electrical Contacts. 2000, New York: IEEE. 225-230.
3. O. Nilsson, F. Hauner, D. Jeannot, Replacement of AgCdO by $AgSnO_2$ in DC contactors[C]. Proceedings of the 50th IEEE Holm Conference on Electrical Contacts/the 22nd International Conference on Electrical Contacts. 2004, New York: IEEE. 70-74.
4. S. Gavriliu, M. Lungu, E. Enescu, S. Nitu, D. Patroi, A comparative study concerning the obtaining and using of some Ag-CdO, Ag-ZnO and Ag-SnO_2 sintered electrical contact materials[J], Optoelectronics and Advanced Materials-Rapid Communications, 2009, **3**(7): 688-692.
5. B. Rehani, P. B. Joshi, P. K. Khanna, Fabrication of silver-graphite contact materials using silver nanopowders[J], Journal of Materials Engineering and Performance, 2010, **19**(1): 64-69.
6. J. Swingler, Performance and arcing characteristics of Ag/Ni contact materials under DC resistive load conditions[J], IET Science, Measurement & Technology, 2011, **5**(2): 37-45.
7. H. Zhang, X. H. Wang, Y. P. Li, C. S. Guo, C. M. Zhang, Preparation and characterization of slver-doped graphene-reinforced silver matrix bulk composite as a novel electrical contact material[J], Applied Physics A, 2019, **125**(2): 1-9.
8. Z. M. Sun, Progress in research and development on MAX phases: a family of layered ternary compounds[J], International Materials Reviews, 2011, 56(3): 143-166.
9. G. M. Zheng, Z. Y. Huang, Q. Yu, W. Q. Hu, X. Y. Qiu, A. Lixia, Y. B. Wang, Y. D. Jiao, Y. Zhou, H. X. Zhai, Microstructural and mechanical properties of TiC_x-Ni_3(Al, Ti)/Ni functionally graded composites fabricated from Ti_3AlC_2 and Ni Powders[J], Metals and Materials International, 2019, 1-9.
10. X. H. Wang, Y. C. Zhou, Layered machinable and electrically conductive Ti_2AlC and Ti_3AlC_2 ceramics: a review[J], Journal of Materials Science & Technology, 2010, 26(5): 385-416.

11. J. X. Ding, W.B. Tian, P. G. Zhang, M. Zhang, Y. M. Zhang, Z. M. Sun, Arc erosion behavior of Ag/Ti_3AlC_2 electrical contact materials[J], Journal of Alloys and Compounds, 2018, 740: 669-676.
12. J. X. Ding, W. B. Tian, P. G. Zhang, M. Zhang, J. Chen, Y. M. Zhang, Z. M. Sun, Preparation and arc erosion properties of Ag/Ti_2SnC composites under electric arc discharging[J], Journal of Advanced Ceramics, 2019, 8(1): 90-101.
13. J. X. Ding, P. Y. Huang, Y. H Zha, D. D. Wang, P. G. Zhang, W. B. Tian, Z. M. Sun, High-purity Ti_2AlC powder: preparation and application in Ag-based electrical contact materials[J], Journal of Inorganic Materials, 2020, 35(6): 729-734.
14. J. X. Ding, W. B. Tian, D. D. Wang, P. G. Zhang, J. Chen, Z. M. Sun, Arc erosion and degradation mechanism of Ag/Ti_2AlC composite[J], Acta Metallurgica Sinica, 2019, 55(5): 627-637.
15. J. X. Ding, W. B. Tian, D. D. Wang, P. G. Zhang, J. Chen, Y. M. Zhang, Z. M. Sun, Microstructure evolution, oxidation behavior and corrosion mechanism of Ag/Ti_2SnC composite during dynamic electric arc discharging[J], Journal of Alloys and Compounds, 2019, 785: 1086-1096.
16. Y. M. Gong, W. B. Tian, P. G. Zhang, J. Chen, Y. M. Zhang, Z. M. Sun, Slip casting and pressureless sintering of Ti_3AlC_2[J], Journal of Advanced Ceramics, 2019, 8: 367-376.
17. X. C. Huang, Y. Feng, G. Qian, K. Liu, Erosion behavior of Ti_3AlC_2 cathode under atmosphere air arc[J], Journal of Alloys and Compounds, 2017, 727: 419-427.
18. X. C. Huang, Y. Feng, G. Qian, J. C. Zhang, X. B. Zhang, Influence of breakdown voltages on arc erosion of a Ti_3AlC_2 cathode in an air atmosphere[J], Ceramics International, 2017, 43(13): 10601-10605.
19. X. C. Huang, Y. Feng, G. Qian, H. Zhao, Z. K. Song, J. C. Zhang, X. B. Zhang, Arc corrosion behavior of Cu-Ti_3AlC_2 composites in air atmosphere[J], SCIENCE CHINA Technological Sciences, 2018, 61(4): 551-557.
20. M. M. Liu, J. L. Chen, H. Cui, X. D. Sun, S. H. Liu, M. Xie, Ag/Ti_3AlC_2 composites with high hardness, high strength and high conductivity[J], Materials Letters, 2018, 213: 269-273.
21. M. Liu, J. Chen, H. Cui, S. Liu, X. Sun, M. Xie, X. Li, Temperature-driven deintercalation and structure evolution of Ag/Ti_3AlC_2 composites[J], Ceramics International, 2018, 44(15): 18129-18134.
22. J. X. Ding, W. B. Tian, D. D. Wang, P. G. Zhang, J. Chen, Y. M. Zhang, Z. M. Sun, Corrosion and degradation mechanism of Ag/Ti_3AlC_2 composites under dynamic electric arc discharging[J], Corrosion Science, 2019, 156: 147-160.
23. M. Naguib, M. Kurtoglu, V. Presser, J. Lu, J. Niu, M. Heon, L. Hultman, Y. Gogotsi, M. W. Barsoum, Two-dimensional nanocrystals produced by exfoliation of Ti_3AlC_2[J], Advanced Materials, 2011, 23(37): 4248-4253.
24. B. Anasori, M. R. Lukatskaya, Y. Gogotsi, 2D metal carbides and nitrides(MXenes) for energy storage[J], Nature Reviews Materials, 2017, 2(2): 16098.

25. M. Naguib, J. Come, B. Dyatkin, V. Presser, P. L. Taberna, P. Simon, M. W. Barsoum, Y. Gogotsi, MXene: a promising transition metal carbide anode for lithium-ion batteries[J], Electrochemistry Communications, 2012, 16(1): 61-64.
26. W. Zheng, P. Zhang, J. Chen, W. B. Tian, Y. M. Zhang, Z. M. Sun, In situ synthesis of CNTs@Ti_3C_2 hybrid structures by microwave irradiation for high-performance anodes in lithium ion batteries[J], Journal of Materials Chemistry A, 2018, 6(8): 3543-3551.
27. F. Shahzad, M. Alhabeb, C. B. Hatter, B. Anasori, S. Man Hong, C. M. Koo, Y. Gogotsi, Electromagnetic interference shielding with 2D transition metal carbides(MXenes)[J], Science, 2016, 353(6304): 1137-1140.
28. X. F. Yu, Y. C. Li, J. B. Cheng, Z. B. Liu, Q. Z. Li, W. Z. Li, X. Yang, B. Xiao, Monolayer Ti_2CO_2: a promising candidate for NH_3 sensor or capturer with high sensitivity and selectivity[J], ACS Applied Materials & Interfaces, 2015, 7(24): 13707-13713.
29. H. Zhang, L. Wang, Q. Chen, P. Li, A. Zhou, X. Cao, Q. Hu, Preparation, mechanical and anti-friction performance of MXene/polymer composites[J], Materials & Design, 2016, 92: 682-689.
30. J. C. Lei, X. Zhang, Z. Zhou, Recent advances in MXene: preparation, properties, and applications[J], Frontiers of Physics, 2015, 10(3): 276-286.
31. V. M. H. Ng, H. Huang, K. Zhou, P. S. Lee, W. X. Que, J. Z. Xu, L. B. Kong, Recent progress in layered transition metal carbides and or nitrides(MXenes) and their composites-synthesis and applications[J], Journal of Materials Chemistry A, 2017, 5(7): 3039-3068.
32. Y. P. Wang, H. Y. Li, Improved workability of the nanocomposited $AgSnO_2$ contact material and its microstructure control during the arcing process[J], Metallurgical and Materials Transactions A, 2017, 48(2): 609-616.
33. I. R. Shein, A. L. Ivanovskii, Graphene-like titanium carbides and nitrides $Ti_{n+1}C_n$, $Ti_{n+1}N_n$(n=1, 2, and 3) from de-intercalated MAX phases: First-principles probing of their structural, electronic properties and relative stability[J], Computational Materials Science, 2012, 65: 104-114.
34. M. Naguib, V. N. Mochalin, M. W. Barsoum, Y. Gogotsi, 25th anniversary article: MXenes: a new family of two-dimensional materials[J], Advanced Materials, 2014, 26(7): 992-1005.
35. M. Naguib, O. Mashtalir, J. Carle, V. Presser, J. Lu, L. Hultman, Y. Gogotsi, M. W. Barsoum, Two-dimensional transition metal carbides[J], ACS Nano, 2012, 6(2): 1322-1331.
36. X. Zhang, S. F. Li, B. Pan, D. Pan, L. Liu, X. D. Hou, M. Q. Chu, K. Kondoh, M. Q. Zhao, Regulation of interface between carbon nanotubes-aluminum and its strengtheningeffect in CNTs reinforced aluminum matrix nanococomposites[J], Carbon, 2019, 155: 686-696.

Figures

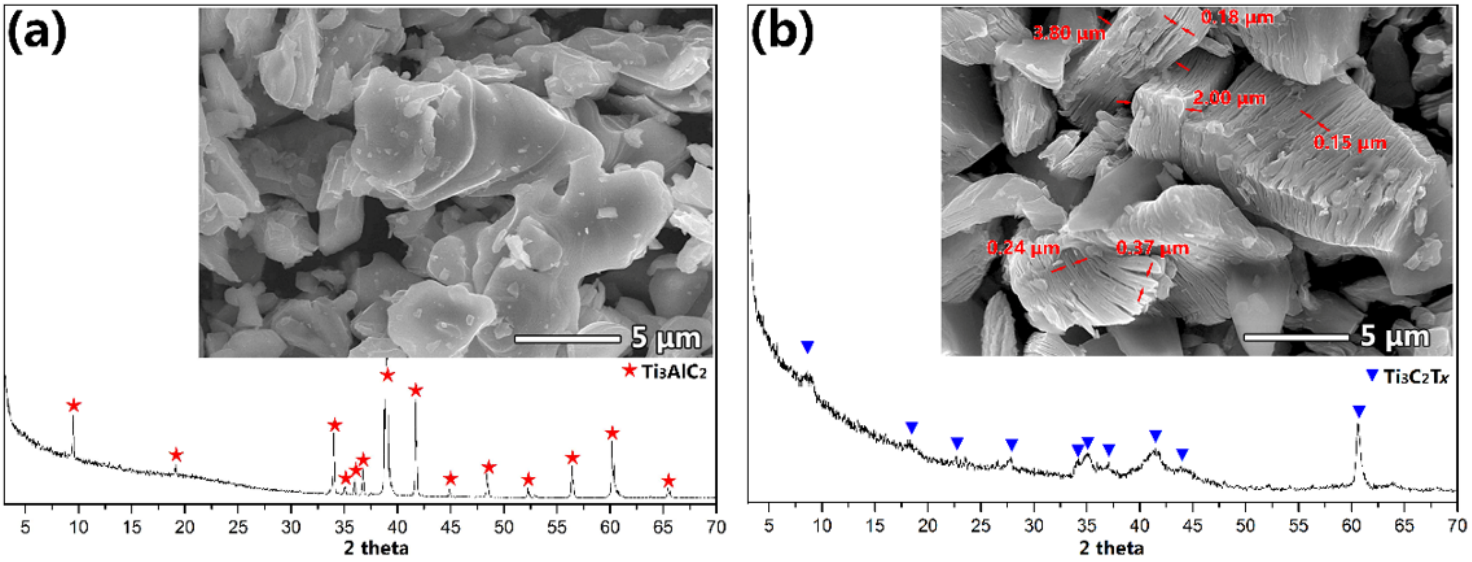

Figure 1

Phase and micro-morphologies of the reinforcing phase: (a)Ti3AlC2; (b)Ti3C2Tx.

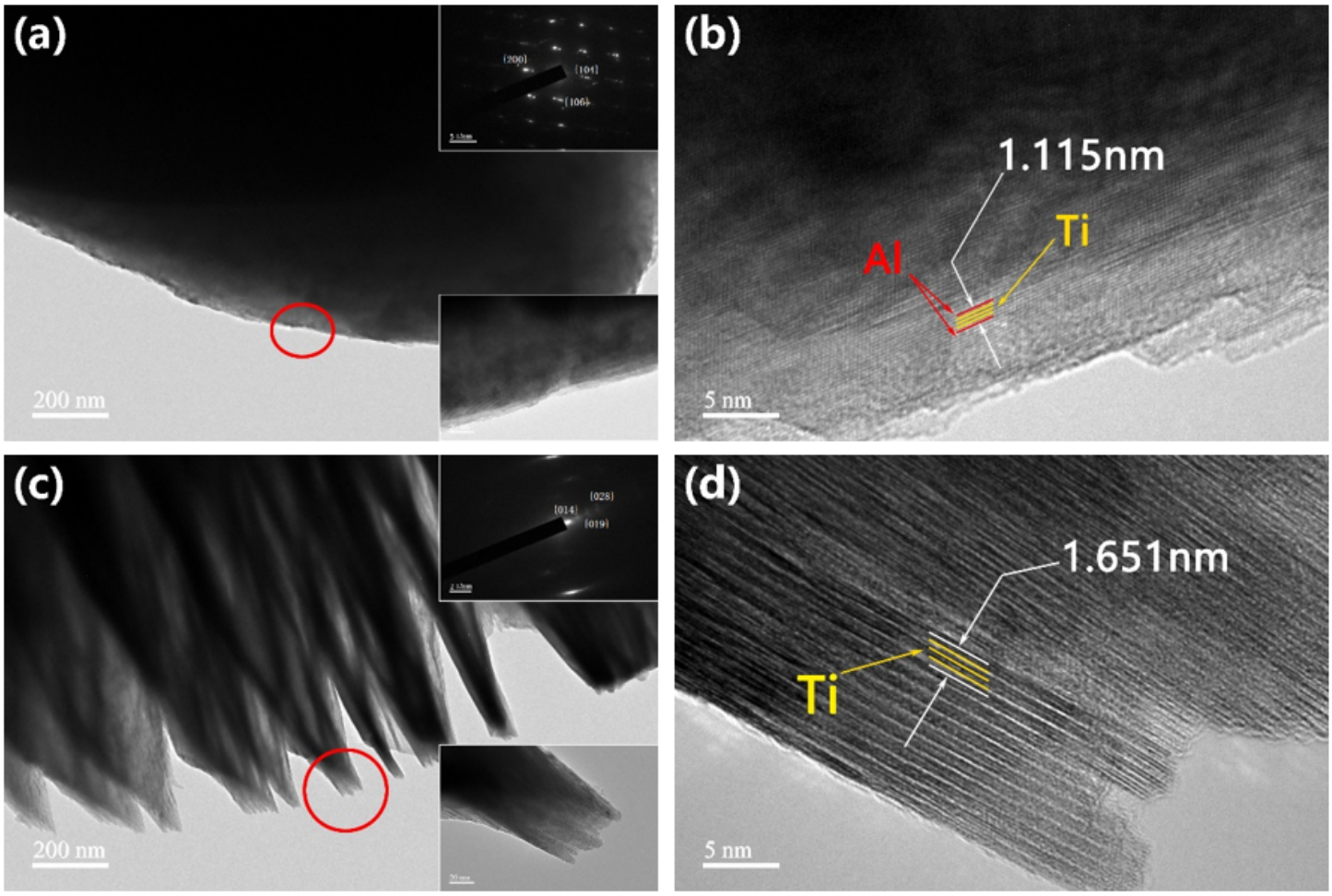

Figure 2

Bright field TEM and selected area electron diffraction(SAED) pattern(inset) of (a)Ti3AlC2 and (c)Ti3C2Tx; high resolution transmission electron microscope(HRTEM) image of (b)Ti3AlC2 and (d)Ti3C2Tx.

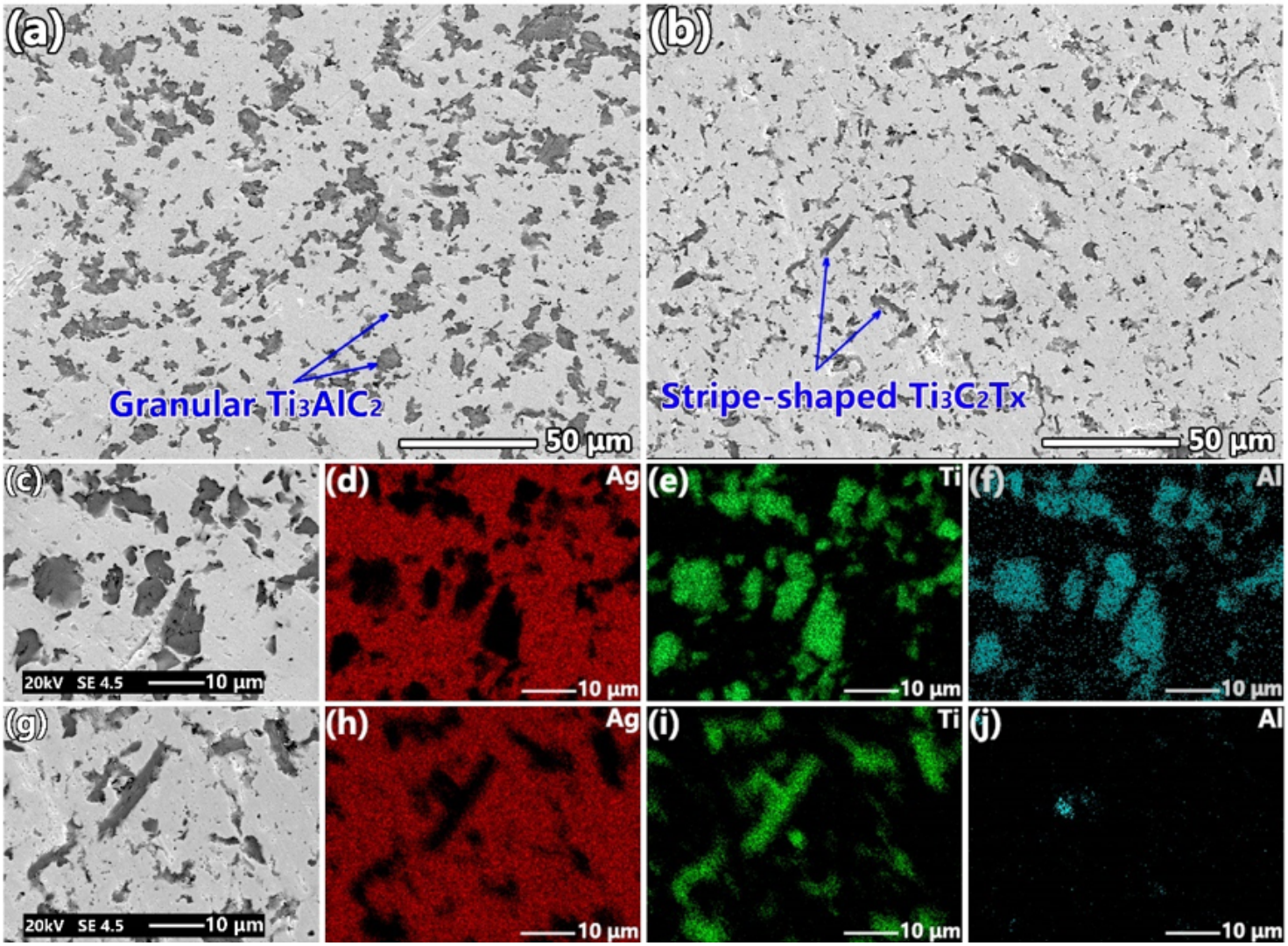

Figure 3

Microstructure of the Ag-based composites, (a)Ag/Ti3AlC2 and (b)Ag/Ti3C2Tx; Element distribution of the Ag-based composites, (c-f)Ag/Ti3AlC2 and (g-j)Ag/Ti3C2Tx.

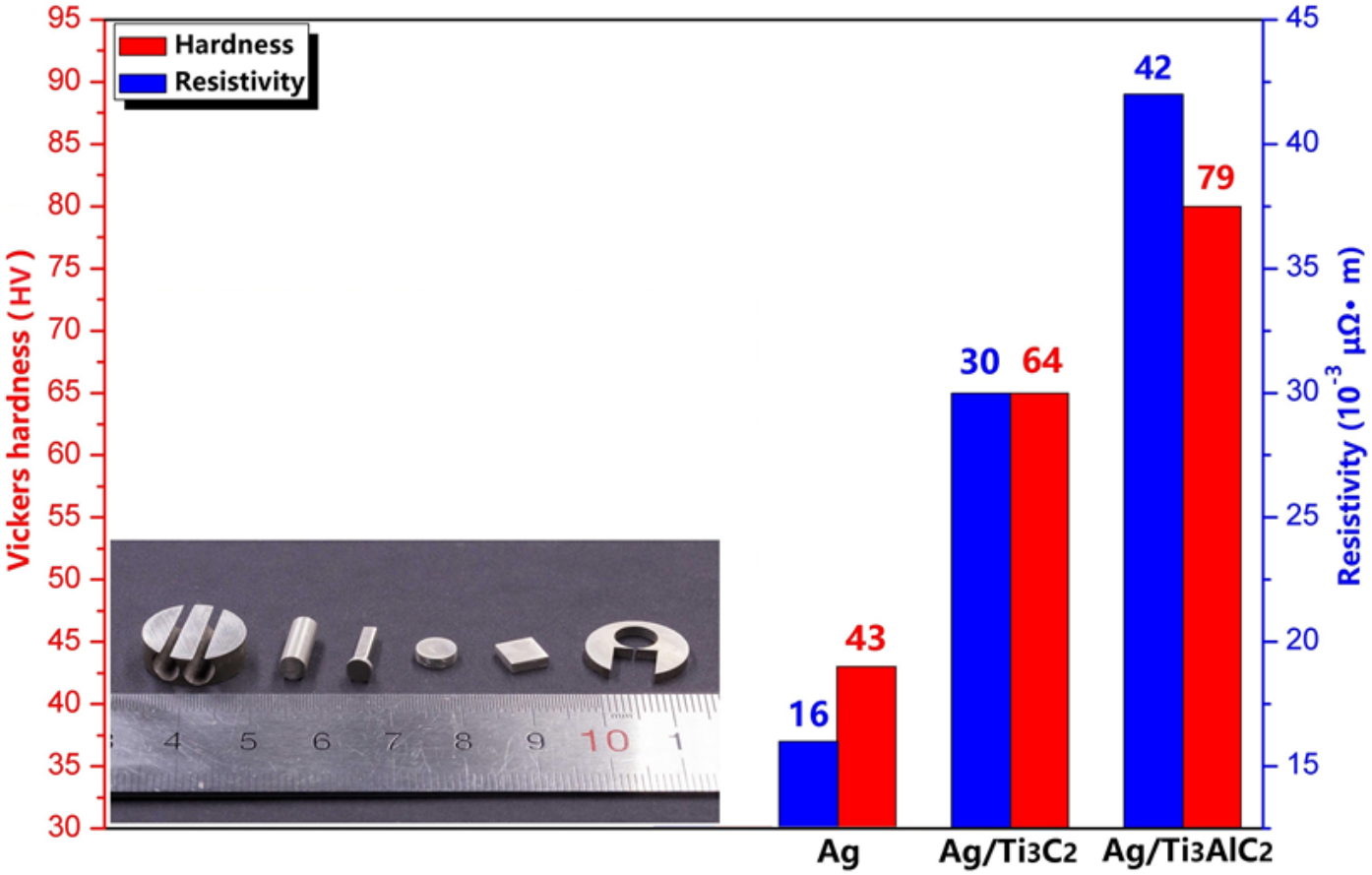

Figure 4

Machinability, electrical resistivity(blue bar) and Vickers hardness(red bar) of Ag/Ti3C2Tx and Ag/Ti3AlC2, compared with those of Ag; the insert: pieces cut from Ag/Ti3C2Tx.

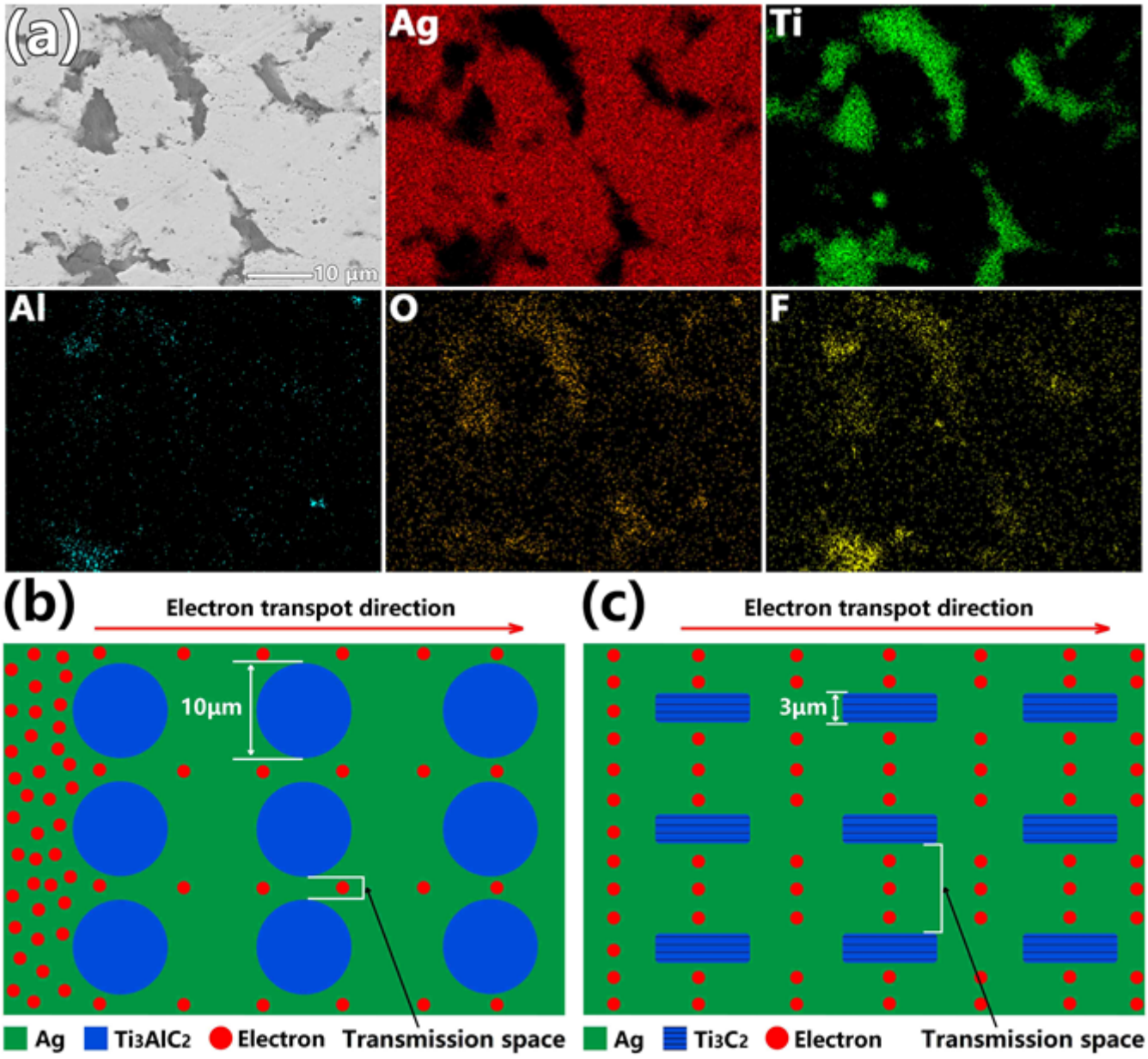

Figure 5

(a) Elements distribution of Ag/Ti3C2Tx composites. (b, c) Schematic illustration of the relationship between the electron transmission and the shape of reinforcements in the composites: (b) Ag/Ti3AlC2 and (c) Ag/Ti3C2Tx.

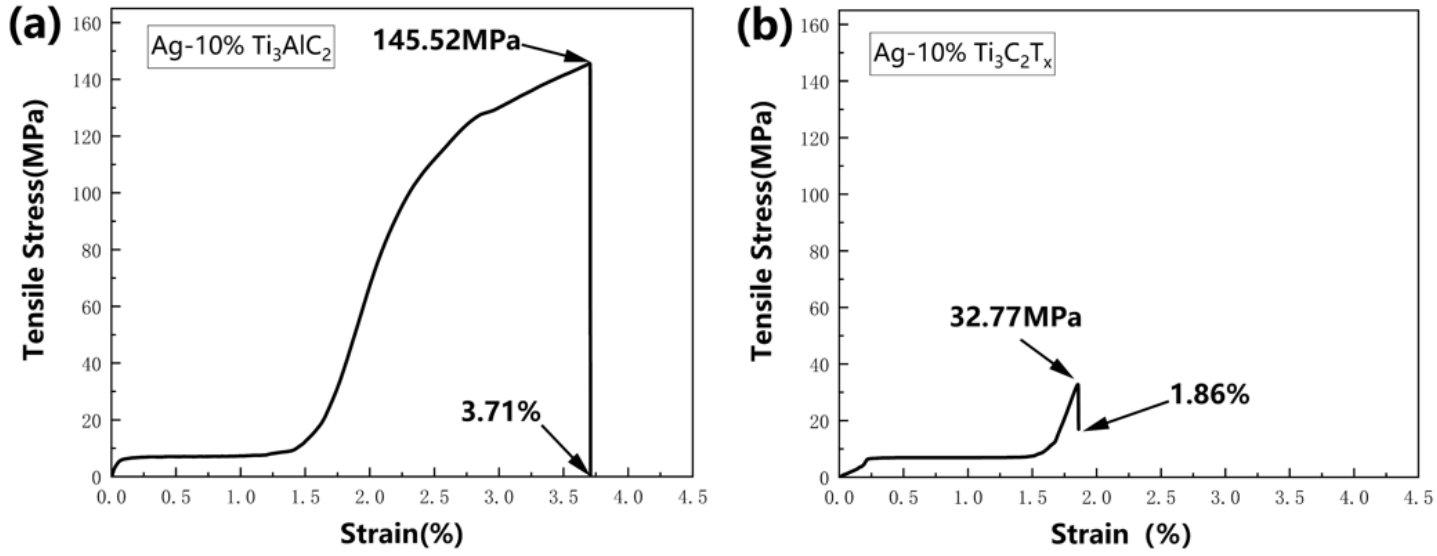

Figure 6

Tensile properties of Ag-based composites reinforced by different materials, (a) Ag/Ti3AlC2 (b) Ag/Ti3C2Tx.

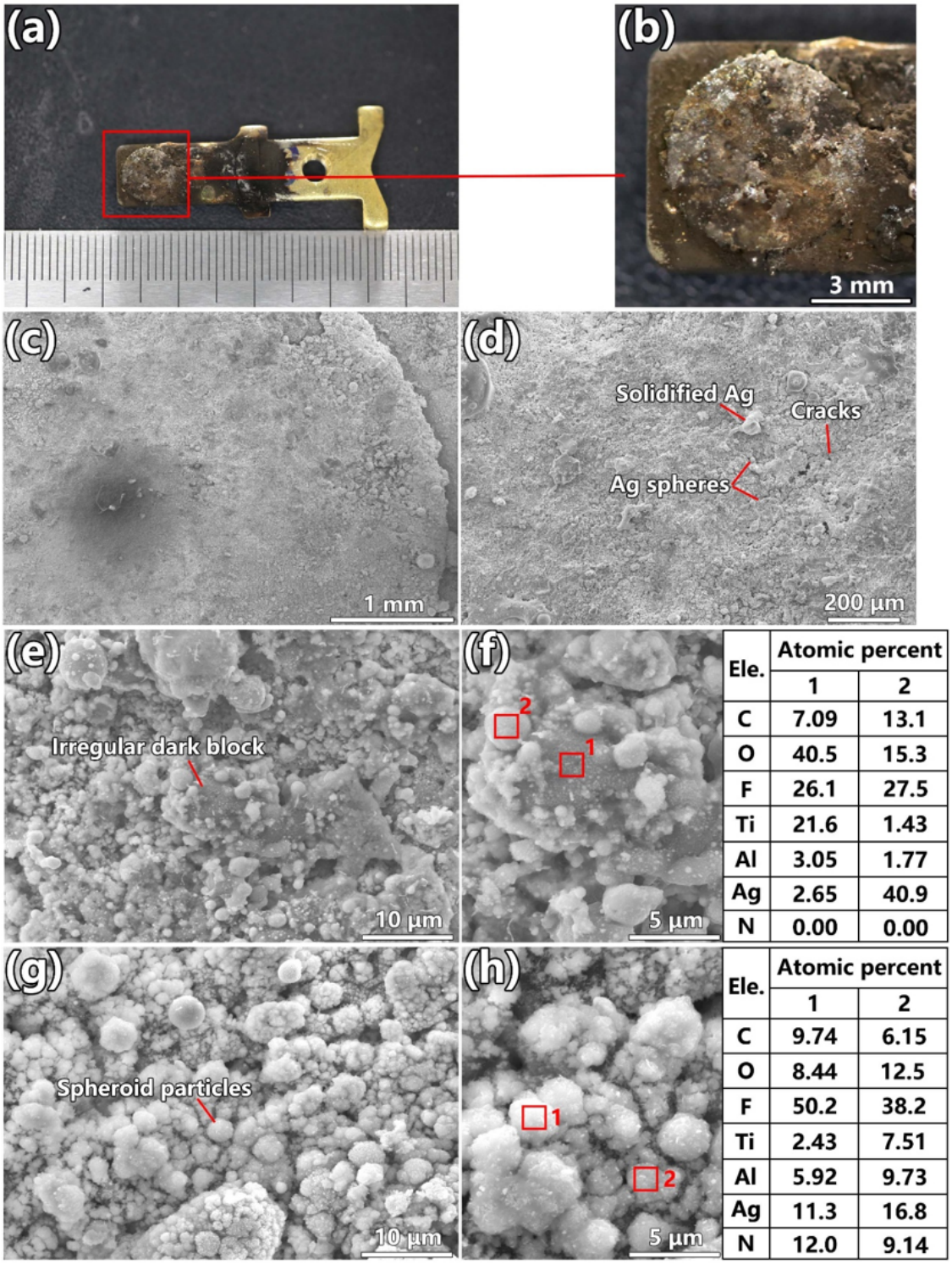

Ele.	Atomic percent	
	1	2
C	7.09	13.1
O	40.5	15.3
F	26.1	27.5
Ti	21.6	1.43
Al	3.05	1.77
Ag	2.65	40.9
N	0.00	0.00

Ele.	Atomic percent	
	1	2
C	9.74	6.15
O	8.44	12.5
F	50.2	38.2
Ti	2.43	7.51
Al	5.92	9.73
Ag	11.3	16.8
N	12.0	9.14

Figure 7

(a,b) Optical images and magnified image of Ag/Ti3C2Tx contact after arc erosion test; (c,d) Surface morphologies of Ag/Ti3C2Tx contact after arc erosion; (e-f) Microstructures and chemical composition of Ag/Ti3C2Tx contact surface after arc erosion.